DUMAND-9-92

Fermilab Library
0 1160 0021415 9

High Energy Neutrino Astrophysics

Potential Sources and their Underwater Detection*

VICTOR J. STENGER
Department of Physics and Astronomy, University of Hawaii
Honolulu, Hawaii 96822, USA

ABSTRACT

At least four underwater high energy neutrino telescopes are now being planned or are already under construction. Procedures for estimating their flux sensitivities are outlined. The generic cosmic beam dump experiment is analyzed, and it is shown that efficient pp production of neutrinos requires matter densities less than 10^{-8} gcm^{-3} and column densities greater than approximately 50 gcm^{-2}. The implication of the observation of γ-rays from active galaxies are discussed. Recent models which predict significant pγ neutrino production from the cores of active galaxies are reviewed and event rate estimates for underwater detectors presented. Other possible very high energy neutrino sources are briefly summarized.

1. Introduction

NESTOR is one of four projects now being planned or already under construction in which a natural body of water will be used as the detection medium for the interactions of very high energy neutrinos (VHE: $E_\nu \geq 100$ GeV) from the cosmos. The others are DUMAND, Baikal, and AMANDA. Reports on DUMAND and Baikal join those on NESTOR in these proceedings.

Of these projects, DUMAND is perhaps the nearest to achieving the goal of detection of very high energy extraterrestrial neutrinos. During the years of its planning and preparation, a considerable amount of effort has gone into estimating the sensitivity of underwater detectors and evaluating potential

---

* To appear in the Proceedings of the 2nd NESTOR International Workshop, 19–22 October, 1992, Pylos, Greece, L. Resvanis, ed.

sources, both specifically and generically. In this report I review the current status of these studies and indicate how this experience may also be applied to NESTOR and the other projects.

2. The Sensitivity of Underwater Detectors

2.1 How to Calculate the Undersea Muon Flux Produced by Very High Energy Neutrinos

The flux of muons above an energy E_μ through a detector located at a depth d resulting from a neutrino flux F_ν can be calculated as illustrated in Fig. 1.

The muon flux is calculated from

$$F_\mu(>E_\mu) = N_A \int_{E_\mu}^{\infty} dE_\nu \frac{dF_\nu}{dE_\nu} e^{-N_A \sigma_T L(\theta)} \int_0^{1-\frac{E_\mu}{E_\nu}} dy\, R_\mu[E_\mu\,,\,(1-y)E_\nu] \frac{d\sigma_\nu}{dy} \tag{1}$$

where

$$L(\theta) = \int_0^{s(\theta)} \rho(r)\, dx \tag{2}$$

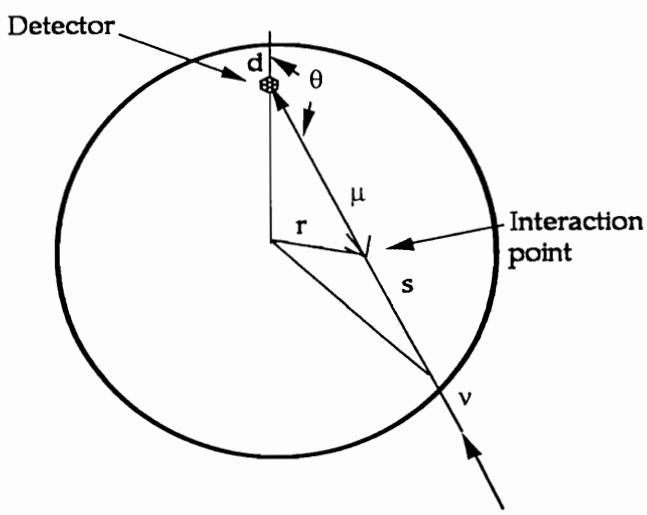

Figure 1 . The path of a neutrino and its produced muon through the earth to the detector.

is the path length traversed by the neutrino through the earth and R_μ is the range of a muon of initial energy $(1-y)E_\nu$ and final energy E_μ. The density of the earth as a function of depth is shown in Fig. 2.

1.2 Event Rates

In order to compute event rates in the

detector, the derivative of the muon flux (1) must be integrated over the effective area of the detector, which, for the underwater projects being considered here, depends sharply on muon energy.

$$N_\mu(>E_\mu) = \int_{E_\mu}^{\infty} \frac{dF_\mu}{dE_\mu} A_{eff}(E_\mu) dE_\mu \tag{3}$$

In the case of DUMAND, $A_{eff}(E_\mu)$ is given in Fig. 3.

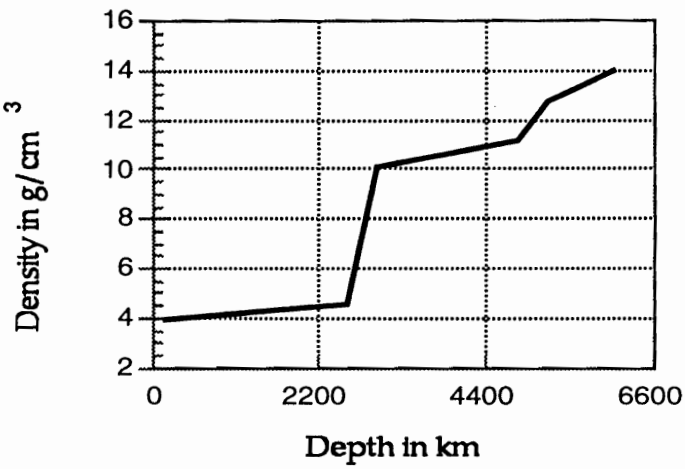

Figure 2 . The density of the earth as a function of depth.

1.3 The Importance of Background Estimates

DUMAND is expected to be signal-limited for point sources of very high energy neutrinos. That is, the array was designed so that a signal of 5–10 events per year in one resolved solid angle element, or pixel, on the celestial sphere can be detected. This requires that all backgrounds in that pixel must be less than one or two events per year. The resolvable pixel area of underwater detectors will depend strongly on muon energy. It also will depend on details of analysis and fitting algorithms. Monte Carlos indicate that, for the anticipated neutrino spectra, a pixel area of π sq. degrees is reasonable. Thus, an underwater neutrino telescope at 4.8 km depth will be able to search for point sources in some 8,000 pixel elements on the celestial sphere, including all upcoming events plus those arriving from up to 20° above the horizon. Since the latitude of Hawaii is 21°, DUMAND can search almost the entire sky at least half of the time.

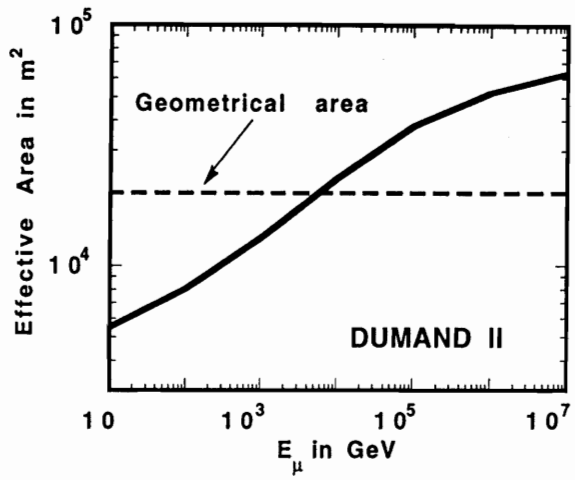

Figure 3. Effective area of DUMAND II as a function of muon energy, averaged over the "signal" region $1<\cos\theta_Z < 0.2$. Also shown is the averaged geometrical area. Above about 5 TeV, events missing the array are often detected.

Estimates of the fake neutrino events expected from the various backgrounds in DUMAND are listed in Table 1. The errors indicated arise from Monte Carlo statistics. These background estimates were made by running simulations of each background type through the same triggering, filtering, and reconstruction algorithms used for estimating the effective area for neutrino signals shown in Fig. 3.[1] The flux sensitivities quoted here are based on a realistic assessment of backgrounds and signal-to-noise.

Table 1. Backgrounds in DUMAND.

K^{40} and other random noise	0.40 ± 0.08 y^{-1} $pixel^{-1}$
Single cosmic ray muons	0.63 ± 0.36
Multiple cosmic ray muons	0.15 ± 0.07
Atmospheric neutrinos	0.13 ± 0.01
Total	1.31 ± 0.38

Note from Table 1 that, even at 4.8 km, cosmic rays are the greatest background. It should be remarked that those experiments which will be located at far shallower depths than

DUMAND or NESTOR, in particular Baikal and AMANDA, will have much greater difficulty dealing with the cosmic ray background. In the case of AMANDA, which will be located in polar ice, the absence of K^{40} will help; but it is still very likely that severe cuts will be necessary that will reduce the effective area and angular acceptance substantially from what would be possible with the same array at greater depths.

If one simply scales up the cosmic ray backgrounds listed above by the approximate factor of 500 that the cosmic ray flux at 1 km exceeds that at 4.8 km, we get almost 400 fake events per year per pixel for a detector equivalent to DUMAND located at 1 km depth. In order to detect a signal at the 5σ level in the presence of this background, some 100 events would then be required. That is, if DUMAND were deployed at 1 km, it would be inherently an order of magnitude less sensitive than the same instrument deployed at 4.8 km.

For these reasons, the sensitivity estimates given here should not simply be scaled by detection area to determine the sensitivities for other underwater instruments, unless all the cuts needed to reduce the background per pixel to negligible proportions have been implemented in the estimation of that detection area.

1.4 Detectability of VHE Neutrino Point Sources

Let us first consider a generic neutrino point source with an E_ν^{-2} differential spectrum. As Kazanas pointed out at this workshop, such spectra are expected for a wide class of objects, corresponding to the situation in which the source emits equal power per decade. Then, using the procedures and caveats outlined above, an underwater detector with a geometrical area averaged over zenith angle of 20,000 m^2 will be able to detect, in one year's observation, a source with a neutrino flux greater than

$$1.2\times10^{-10} \text{ neutrinos cm}^{-2}\,\text{s}^{-1}$$

at energies greater than 1 TeV. (Note that this is not meant to imply that the detector has a threshold of 1 TeV; this is merely taken as a handy reference point.)

This result is to be compared with the γ–ray fluxes that have been observed by the Whipple Air Cherenkov experiment for the two sources that have been convincingly detected at these energies:[2,3]

Crab Nebula:	2.5×10^{-11} photons $cm^{-2}\ s^{-1}$
Markarian 421:	7.5×10^{-12} photons $cm^{-2}\ s^{-1}$

Although the Crab is not regarded as a likely neutrino candidate, its observed flux represents about the current sensitivity level of experiments for photons in the TeV energy region. Thus DUMAND, while a factor of 50 more sensitive than previous high energy neutrino telescopes, will not quite achieve a sensitivity in neutrinos equivalent to the photon sensitivity of VHE γ–ray telescopes. Another factor of five is needed, or $10^5\ m^2$ – which is what is being planned for NESTOR and the next stage of DUMAND.

Comparing neutrino and photon sensitivities is relevant since any observed sources of VHE γ–rays would be likely candidates for neutrinos, assuming hadronic processes are the origin of the photons. As we will see in the next section, a factor of five enhancement of neutrinos to photons may be expected under favorable conditions. And in a later discussion, I will show why we expect that detectable neutrino sources exist from which no γ–ray photons reach earth.

1.5 Cascade Detection

The above analysis was solely based on the detection of muons from muon neutrino charge current events. Of course, neutrino events without muons can also be detected by means of their hadronic cascade. Although the level of this analysis has not yet reached the sophistication of the muon analysis, with fully–developed event reconstruction algorithms and background estimations, some event rate estimates have been made and are reported elsewhere.[4]

3.0 Expected Neutrino Fluxes

A considerable literature exists on estimating neutrino fluxes from (1) binary neutron star systems, (2) expanding supernova shells, and (3) active galactic nuclei (AGN). With the lack of confirmation of previously–reported VHE and UHE γ–rays from Cyg X–3, Her X–1, and other binary neutron star systems, class (1) is no longer looking so promising for the next generation of neutrino telescopes, although they will certainly be examined.

No VHE neutrinos or γ–rays were seen from SN1987a.

However, analysis of the lower energy observations from that event has led to an upward revision of the time that the expanding shell of a suitable supernova would be thick enough to act as a efficient beam dump for any protons accelerated by the neutron star left behind. So class (2) remains a serendipitous possibility.

I will later return to a discussion of class (3), the AGNs, which now appear the most intriguing possibility for the detection of VHE neutrinos. Before doing this, however, I would like to outline how an estimate can be made of the scale of neutrino fluxes, or the neutrino to γ–ray flux ratio, in a generic manner that does not depend on any specific model or precise details of the source characteristics.

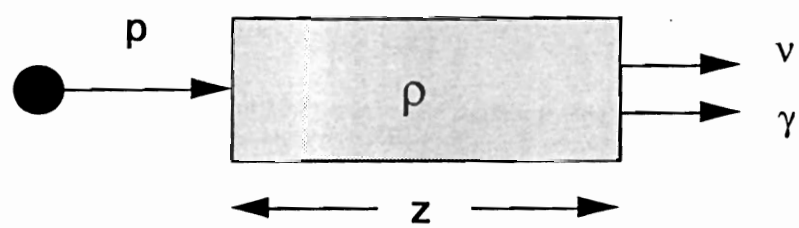

Figure 4 . Illustration of cosmic beam dump experiment.

3.1 A Cosmic Beam Dump Experiment

Suppose a source of protons with a power–law spectral emission given by

$$N_p(E_p) = N_p(1)\, E_p^{-\alpha} \tag{4}$$

protons s^{-1} TeV^{-1}, where E_p is in TeV, strikes a column of matter of uniform density ρ gcm^{-3} and column density z gcm^{-2}, as shown in Fig. 4. Assuming pp collisions, the emission of neutrinos and γ–rays can be numerically calculated as the decay products of the pions and other hadrons produced in the primary interaction, plus any secondaries that may also be generated. These can be expressed in terms of "efficiencies" ε_ν and ε_γ as follows:

$$N_\nu(E_\nu, \rho, z, \alpha) = \varepsilon_\nu\, N_p(E_\nu) \tag{5}$$

$$N_\gamma(E_\gamma, \rho, z, \alpha) = \varepsilon_\gamma\, N_p(E_\gamma) \tag{6}$$

where the proton spectrum has been integrated from E_ν to ∞.

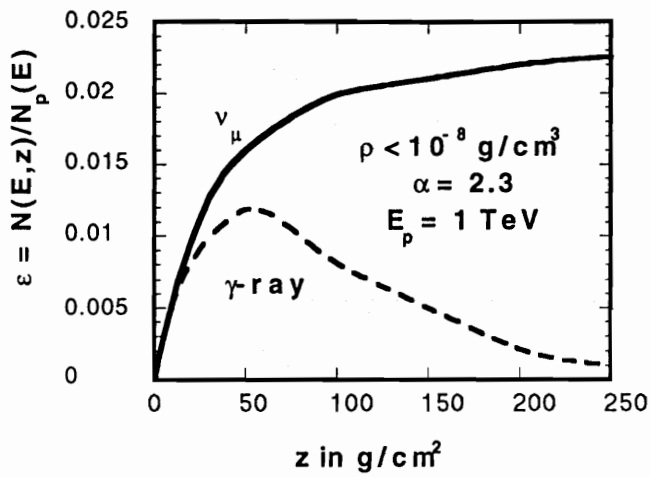

Figure 5. The efficiency for muon neutrino (solid) and γ–ray (dashed) emission at 1 TeV as a function of column density z in a cosmic beam dump experiment. The matter density $\rho \leq 10^{-8}$ g cm^{-3}.

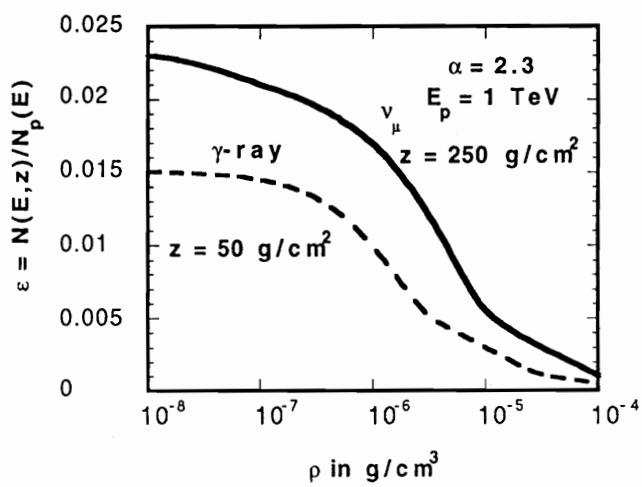

Figure 6. The efficiency for muon neutrino (solid) and γ–ray (dashed) emission at 1 TeV as a function of the matter density ρ in a cosmic beam dump experiment for optimal column densities z of 250 g cm^{-2} for ν_μ and 50 g cm^{-2} for γ.

In Fig. 5, ε_ν and ε_γ at 1 TeV are shown is a function of z for $\rho \leq 10^{-8}$ gcm^{-3} and $\alpha = 2.3$. Above 10^{-8} gcm^{-3}, pions and kaons have a chance of interacting before decaying, and the flux of both neutrinos

and γ–rays are reduced. The effect is shown in Fig. 6. Here optimum column densities of 250 gcm^{-2} for neutrinos and 50 gcm^{-2} for γ–rays were chosen for illustration.

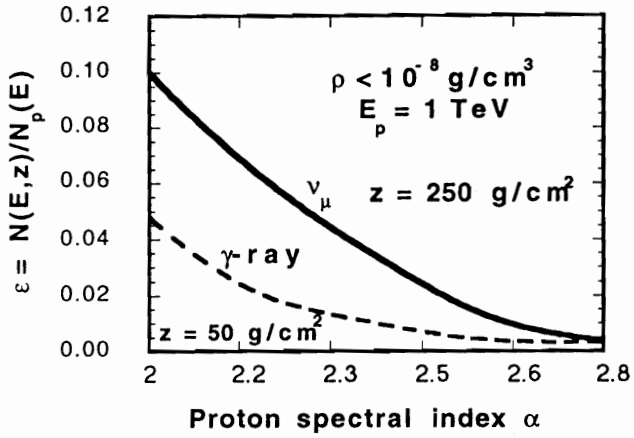

Figure 7 The efficiencies for muon neutrino (solid) and γ–ray (dashed) emission spectra expected as a function of proton spectral index α for the optimum matter and column densities indicated.

The calculations which produced the above results also show that the spectra of γ–rays and neutrinos with $\rho \lesssim 10^{-8}$ gcm^{-3} closely follow that of the incident protons. However, the neutrino spectrum steepens as the density increases beyond this amount. Since underwater detectors are less sensitive to steep neutrino spectra, and the neutrino flux is also suppressed, cosmic bean dumps denser than 10^{-8} gcm^{-3} are not promising neutrino sources.

The dependence on proton spectral index is shown in Fig. 7, again where optimum column densities are used. Clearly, the flatter the proton spectrum, the better. This analysis of a generic beam dump experiment allows us to draw some conclusions about the neutrinos and γ–rays we might expect from hadronic pp processes. First, as already emphasized, the density of the matter in the beam dump must be low, $\lesssim 10^{-8}$ gcm^{-3}. Second, we need considerable column density for significant neutrino production, perhaps 50–100 gcm^{-2}. Above 50 gcm^{-2} the γ–rays are suppressed, though this depends somewhat on the spectral index α. For a fairly flat spectrum, $\alpha \approx 2$, the electromagnetic cascade of photons will feed upon itself and a considerable flux of lower energy photons will emerge. However, this is not a consideration here where we are interested mainly in the neutrinos and γ–rays above 100 GeV.

Under the most optimal conditions for neutrino production, $z \gtrsim 100\ gcm^{-2}$, $\rho < 10^{-8}\ gcm^{-3}$, $\alpha \leq 2$, we expect $\varepsilon_\nu \approx 0.1$. In this case, a beam dump will emit 1 TeV neutrinos at a rate about 10% of the rate at which protons of that energy strike the source. Under these conditions, the neutrino flux emitted would be at least three times that of γ–rays produced by the same hadronic interactions. At lower column densities, we will have fewer neutrinos at about the same flux level as γ–rays, or lower. Significant pp neutrino production is not expected from denser sources or from those sources in which the total column density along the line of sight to earth is less than the order of 10 gcm^{-2}.

3.2 Estimating the Flux

Given these considerations, two methods are used to obtain a quantitative estimate of the neutrino flux at earth. In the first, we assume we know the proton luminosity L_p ergs s^{-1} decade^{-1} of the source as a function energy and write:

$$N(E_p) = \log(e)\ L_p\ E_p^{-2} = \log(e)\ L_p(1)E_p^{-\alpha} \tag{7}$$

where we assume a power–law spectrum $L_p = L_p(1)E_p^{2-\alpha}$ and again use 1 TeV as a reference point. The neutrino flux at earth, for an isotropic source at a distance D will then be,

$$F_\nu(E_\nu) = \varepsilon_\nu \log(e)\ L_p(1)E_\nu^{-\alpha}\ /\ 4\pi D^2 \tag{8}$$

The integral flux will be

$$F_\nu(>E_\nu) = \varepsilon_\nu \log(e)\ L_p(1)\ E_\nu^{-\alpha+1}\ /\ 4\pi(\alpha - 1)\ D^2 \tag{9}$$

Using F_ν (>1 TeV) = $1.2\times10^{-10}\ cm^{-2}\ s^{-1}$ as detection threshold for a 20,000 m^2 underwater detector, and taking $\alpha = 2$, $\varepsilon_\nu = 0.1$, we obtain the following expression for the proton luminosity required to be emitted isotropically from a point source to be detected:

$$\log(L_p\ /\ \text{ergs}\ s^{-1}) = 28.6 + 2\log(D\ /\ \text{pc}) \tag{10}$$

In Fig. 8 this is plotted as a function of D, with two horizontal bands that indicate the source luminosities for galactic and extra–galactic objects, where these are taken to be equal to the Eddington luminosity

$$L_{Edd} = 10^{38} \text{ ergs s}^{-1} \ (M/M_{Sun}) \tag{11}$$

with $M = M_{Sun}$ is assumed for the former and $M = 10^8 M_{Sun}$ assumed for the latter. All sources above the solid diagonal are detectable in this model. However, the dashed line indicates current observational limits, indicating that these objects are either not producing protons at the Eddington limit or neutrino production is not optimized and $\varepsilon_\nu < 0.1$.

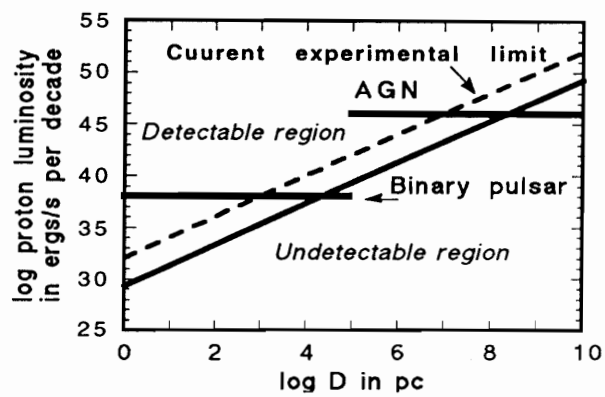

Figure 8. The proton luminosity required for neutrino detection of a point source at a distance D in DUMAND II (solid diagonal line). Luminosities above this line are detectable, The dashed line shows current observational limits. The horizontal bars indicate the Eddington luminosities for galactic objects with mass equal to that of the sun, and extragalactic objects of 10^8 solar masses.

As an alternative method for estimating an expected neutrino flux, we can take the observed γ–ray flux from some source and use it to give

$$F_\nu(E_\nu) = F_\gamma(E_\nu)\, \varepsilon_\nu / \varepsilon_\gamma \tag{12}$$

If we assume a fairly conservative $\varepsilon_\nu / \varepsilon_\gamma = 3$ and the Whipple flux for Mrk 421 mentioned earlier, we get F_ν (>1 TeV) $=7.5\times10^{-12}$ cm^{-2}s^{-1} or about 0.6 events per year from this source in DUMAND or its equivalent. This leads me naturally to my next topic, which is . . .

4. Neutrinos from Active Galaxies

Two recent developments, one experimental and the other theoretical, have caused Active Galaxies to become the prime prospect for VHE neutrinos in DUMAND and the other new generation detectors. I will discuss each in turn.

4.1 Implications of GRO and Whipple Observations

At this writing, the Gamma Ray Observatory (GRO) satellite has reported 14 observations of γ–rays in the 50 MeV – 5 GeV region from identified extragalactic objects with its EGRET and COMPTEL instruments.[5] The brightest so far is the optically violent variable quasar 3C279.[6] The GRO sources, 10 quasars and 4 BL Lac objects, fall in the class of active galaxies known as *blazars* that have always been regarded as prime candidates for γ–rays.[7] Blazars are believed to be quasars or other active galaxies that have their jets more–or–less aligned toward earth. If proton acceleration is, as seems plausible, directed along the jets, then γ–rays and perhaps neutrinos should be seen from these objects. As already noted, the Whipple observatory has reported γ–rays ≳500 GeV from Mrk 421, though they failed to detect 3C279.

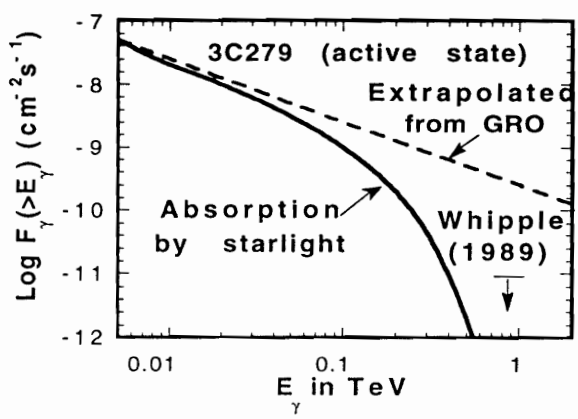

Figure 9 . Extrapolated GRO γ–ray spectrum for 3C279 (dashed) and the spectrum expected from absorption by starlight (solid). Also shown is the Whipple experimental limit. (From Reference 7).

The GRO result on 3C279 (redshift 0.538) shows an E^{-2} spectrum, with the luminosity in γ–rays during the source's bright phase greater than that seen in the radio, visible, or X–ray bands. A straight extrapolation to 1 TeV predicted a signal 2–3 orders of magnitude above the limit set by Whipple. Stecker, De Jager, and Salamon have

argued that a sharp cutoff in the γ–ray spectrum above about 100 GeV will occur for 3C279, and the other distant objects, as the result of scattering from starlight.[8] This could explain the failure of Whipple to see γ–rays from 3C2793, as seen in Fig. 9, and the surprising fact that the first and, so far, only GRO source seen at TeV energies is Mrk 421, the weakest of the GRO sources, 50 times weaker than 3C279, but also the closest, with a redshift 0.031.

Of course, neutrinos will not suffer from this absorption. If we again assume $\nu \approx \gamma$, the GRO flux extrapolated to 1 TeV implies a neutrino event rate of 20 per year in DUMAND. It should be noted however, that the 3C279 flux is variable and the above estimate is based in the high state, which may not last for as long as a year.

4.2 Dumping on Photons

The observations of γ–rays from AGNs by GRO and Whipple may or may not be related to recent models that suggest strong neutrino production from the centers of active galaxies. Early work by Berezinsky; Eichler and Schramm; Silberberg and Shapiro; and Scott, Vestrand, Marscher and Christiansen[9] suggested that AGNs are a possible source for VHE neutrinos. More recently, Stecker, Done, Sommers, and Salamon, were able to make this idea more quantitatively reliable by taking advantage of the latest observational data.[10] The principle is illustrated in Fig.10.

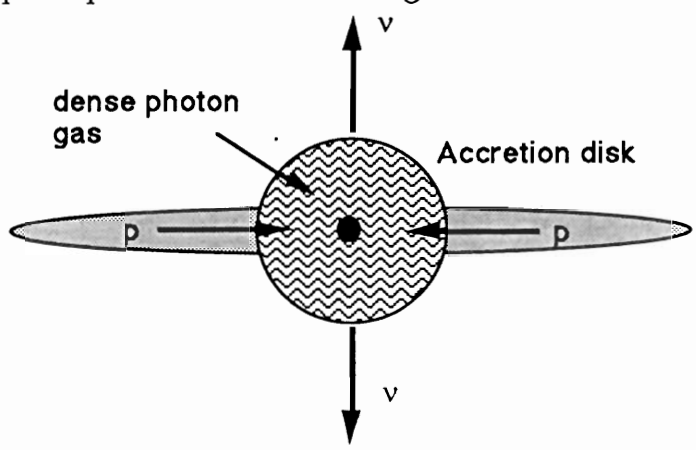

Figure 10. The photon beam dump in AGN central–engine models.

Protons are accelerated by shock waves in the accreting matter around the central black hole, or by some other mechanism. These collide with UV photons in the surrounding medium, producing pions and other mesons which decay to give neutrinos.

The dominant process is

$$
\begin{array}{l}
p\gamma \rightarrow \Delta^{+} \rightarrow \pi^{+} n \\
\qquad\qquad\qquad\quad \downarrow \\
\qquad\qquad\qquad\quad \mu\, \nu_{\mu} \\
\qquad\qquad\qquad\quad \downarrow \\
\qquad\qquad\qquad\quad e\, \nu_{e} \\
\qquad\qquad\qquad \rightarrow \pi^{o} p \\
\qquad\qquad\qquad\quad \downarrow \\
\qquad\qquad\qquad\quad 2\gamma
\end{array}
$$

where $E_p = 10^{16}\,(E_\gamma\,/\,40\text{ eV})$ eV. These objects are characterized by a "UV-bump" at about 40 eV.

The photons produced by π^o decay cascade to lower energies by electromagnetic processes, appearing eventually as X-rays. If it is assumed that the X-ray background is primarily from AGNs, the observed X-ray flux can be used to normalize the calculation of the neutrino flux. The result from the original paper by Stecker et al. implied neutrino event rates so great that they should have been detectable in the larger existing underground experiments, Kamiokande and IMB.

4.3 Expected Fluxes and Event Rates from all AGNs

Spurred by this remarkable prediction, several other groups of astrophysicists developed their own AGN central-engine models, while underground experiments have looked at their data for an AGN signal. In March, 1992, a workshop was held at the University of Hawaii in which the AGN models were critically reviewed and experimental results were reported. At that meeting is was realized that the Stecker et al. flux was over-estimated. Shortly thereafter, Protheroe discovered a typographical error in the paper from which the X-ray background flux was determined. The net effect was to reduce the flux estimate by about a factor of ten. This is consistent with the current observational limits, where no AGN signal is yet reported. The results from several model calculations reported at the Hawaii meeting are shown in Fig. 11

Using the method outlined earlier, the underwater muon flux generated by these neutrinos was calculated. Folding in the DUMAND effective area as a function of muon energy shown in Fig. 3, the event rate estimates integrated over all directions, shown in Fig. 12, were obtained. We see that a signal above atmospheric background of 20–100 events per year is predicted for $E_\mu \gtrsim 5$ TeV.

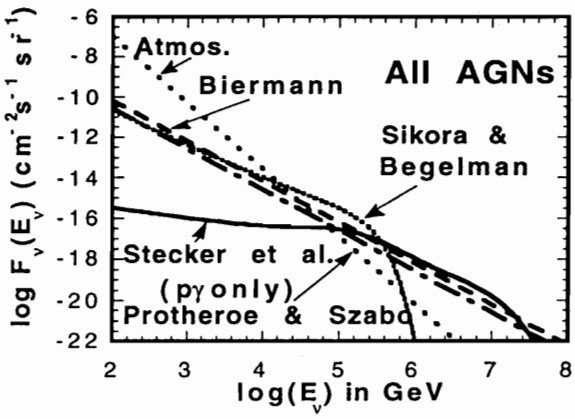

Figure 11 . The total neutrino fluxes from all AGNs according to several models, as reported at the Hawaii workshop. These are to be compared with the background flux of atmospheric neutrinos. Note that Stecker et al. only show the effect of pγ interactions. Other processes fill in the lower energy portion of the spectrum in other models.

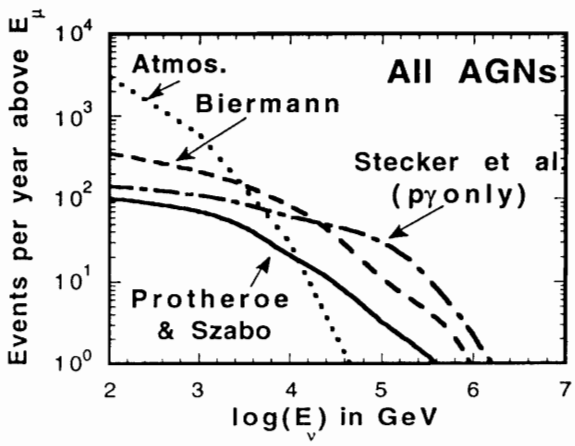

Figure 12 . Event rates above E_μ in DUMAND for the neutrino fluxes given in Fig. 11.

Interestingly, most of the neutrino events come from higher energies. The big difference in the lower energy regions of the spectra in Fig. 11, which, as noted, result from processes other than $p\gamma \rightarrow \Delta$, has only a factor of two or three effect on the signal above 100 GeV. The very flat spectra predicted, compared to the atmospheric background, make it possible to select the signal by a cut on E_μ. As Okada has shown, DUMAND will have sufficient information provided by dE/dx of the

muon to detect the above signal.

Another handle on the detection of a diffuse background of neutrinos from AGNs is provided by the zenith angle distribution, shown in Fig. 13. The effect of absorption of neutrinos in the earth is seen.

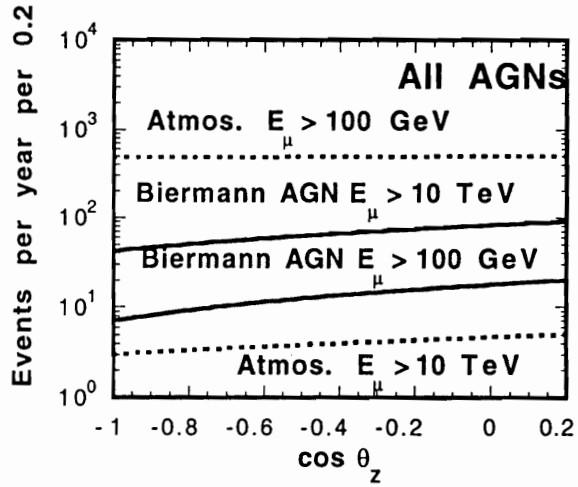

Figure 13 . The zenith angle distribution of AGN events in DUMAND, compared to the atmospheric background, for two cuts in E_μ. The Biermann neutrino flux is used for illustration.

An important by-product of the AGN central-engine model calculations occurred when Protheroe decided to look at the flux of protons that is produced in the outer regions when the neutrons from the central $p\gamma$ reactions decay. With no further input, he found that he could account for almost all the cosmic rays above the "knee" in the spectrum at around 10^{16} eV and below the "ankle" at 10^{19} eV. Thus the observation of neutrinos from AGNs would provide strong confirmation of this hypothesis.

Finally I must add that not all calculations on the central-engine model lead to copious neutrino production. Mastichiadis finds that the proton flux near an AGN would be quenched by runaway electron pair production.[11] This conclusion depends on the magnitude of the magnetic field in the core region and may or may not be a problem.

4.4 Point Source AGNs

Several authors have also made estimates of the neutrino fluxes from several individual AGNs. These are shown in Fig. 14. Again we note the effect of adding other processes besides $p\gamma$. Also note that the

3C279 flux is considerably less than would be expected from a straight-line extrapolation of the GRO observations with the assumption $\nu = \gamma$ (see Fig. 9). The model calculations would seem to suggest that this latter assumption is a bad one, presumably because the column density along the line of sight is less than optimum for neutrino production, although it is to be noted that no γ-rays at all are expected from the core $p\gamma$ processes.

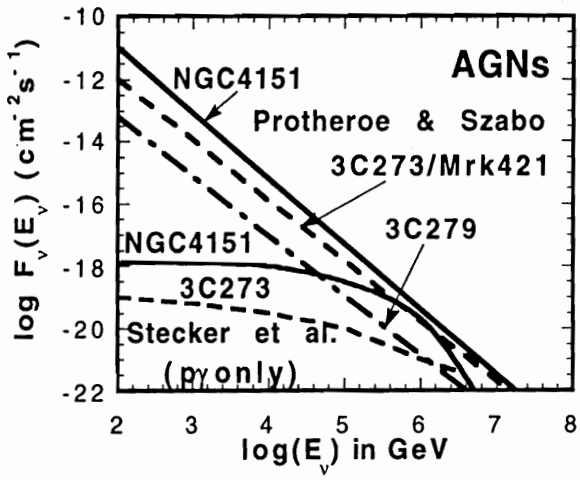

Figure 14 Predicted neutrino flux spectra for several specific AGNs.

4.5 Summary of AGN Event Rates

The event rates expected in DUMAND for the various models is shown in Table 2. The rates from all AGNs are to be compared with the atmospheric background integrated over all zenith angles, which is also shown. The individual source rates should be compared with the point source backgrounds given in Table 1, which are less than 2 events per year per pixel. In these cases, 5–10 events per year with greater than 100 GeV muon energy are detectable.

5. Other Possible Neutrino Sources

Finally I will briefly review the status of estimates on the likelihood that the next generation of VHE neutrino telescopes will see neutrinos from sources other than AGNs.

5.1 Binary Pulsars (Cyg X–2, Her, X–1, etc.)

As mentioned, the failure of previously reported γ-rays from binary pulsars to be confirmed by more sensitive VHE and UHE γ-ray

telescopes has made this class of possible "cosmic accelerators" less promising. However, it should be remarked that several of those earlier reports are hard to argue away and were highly episodic over a decade or more of observation. Binary pulsars certainly remain objects – to be looked at in neutrinos, though the flux levels may require detectors greater than 10^5 m^2.

Table 2. The number of muon events per year expected in DUMAND II from unresolved and resolved AGNs, according to the various independent model calculations. Also shown are the rates expected from two sources observed by GRO, on the assumption that the neutrino flux equals the measured γ–ray flux.

Source	E_μ > 100 GeV	E_μ > 10 TeV	Model
Unresolved AGNs	154	66	Stecker et al.
	109	23	Szabo & Protheroe
	366	75	Biermann
	897	148	Sikora & Begelman
Atmos. ν Bkg	2,950	22.8	Volkova
Resolved AGNs			
NGC 4151	5.0	1.1	Szabo & Protheroe
3C279	0.054	0.013	Szabo & Protheroe
	20.3	4.2	ν = γ (extrap. from GRO)
Mrk 421	0.80	0.197	Szabo & Protheroe
	3.2	0.67	ν = γ (observed at 1 TeV)
3C273	0.80	0.19	Szabo & Protheroe

5.2 Supernova Remnants

Also as mentioned, this remains a serendipitous possibility, despite the non–observation of VHE γ–rays or neutrinos from SN1987a.

5.3 Mini–AGNs in the Galaxy

Sommers has suggested that possible black–hole binary galactic objects, e.g., SS433, may be mini–AGNs.[12] Scaling from AGN calculations, a source luminosity > 5×10^{38} $(D/kpc)^2$ ergs s^{-1} is required for a detectable neutrino flux in DUMAND. For SS433 at 5 kpc, this implies

$L > 10^{40}$ ergs s^{-1}. A $10M_{Sun}$ black hole radiating at its Eddington luminosity of 10^{39} ergs s^{-1} is detectable at $D < 1.4$ kpc.

5.4 γ–Ray Bursters

Making the unfounded assumptions that the observed spectrum of γ–ray bursters extends to the TeV region and $\nu \approx \gamma$, one burst would produce 0.075 events in a 100 s burst period. While not individually detectable, such sources would be detectable statistically.

5.5 WIMPS

Some possibility exists for the detection of neutrinos from WIMPS (SUSY neutralinos) annihilating in the sun or earth.[13] Negative results with large area neutrino detectors will rule out significant portions of SUSY parameter space.[14]

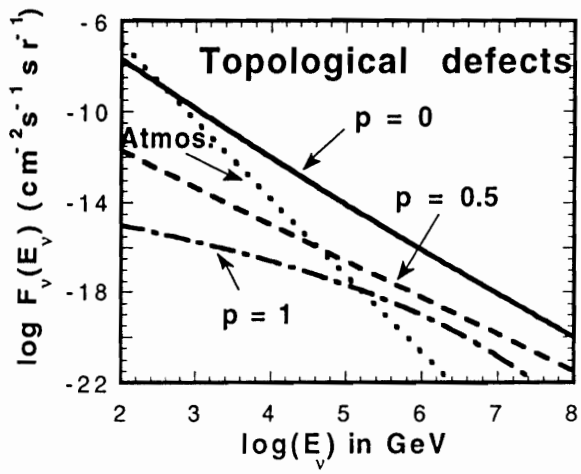

Figure 15. Neutrino fluxes from topological defects in the model of Bhattacharjee, Hill, and Schramm.

5.5 Cosmic Strings or other Topological Defects

Though highly speculative at this stage of knowledge, the annihilation of topological defects would be characterized by considerable neutrino production. The neutrino fluxes from one model in which defect annihilation is normalized to the cosmic ray spectrum above 10^{19} eV is shown in Fig. 15.[15] The parameter p indicates the type of defect. The prediction labelled p = 0, which corresponds to "superconducting cosmic string loops" is already ruled out. Defects with $p \approx 1$, "collapsing cosmic string loops" would be undetectable in

neutrinos. However, defects with $p \approx 0.5$ would be detectable in this model.

6.0 Conclusions

☆ Underwater neutrino telescopes now being planned or under construction will be one or two orders more sensitive than existing underground detectors. However, those at shallow depths must contend with the greater cosmic ray background. Experiments like DUMAND and NESTOR at >4 km will have a neutrino flux sensitivity of 1.2×10^{-10} neutrinos $cm^{-2}\ s^{-1}$ for a geometrical area of 20,000 m^2 averaged over direction, for muon detection.

☆ Cosmic beam dumps which produce neutrinos by pp production must have matter densities $< 10^{-8}\ gcm^{-3}$ and column densities $\gtrsim 50\ gcm^{-2}$ for optimum neutrino production. In that case, the efficiency for neutrino production is about 10% for an E_p^{-2} proton spectrum.

☆ Central engine AGN models in which neutrinos are produced by $p\gamma$ interactions predict measurable ν_μ events above atmospheric background for $E_\mu > 10$ TeV. Differences between models may be detectable, giving information about the energy source. Some individual AGNs may be detectable.

☆ GRO AGN sources are good candidates for ν_μ signals The closest source, Mrk 421, is seen in TeV γ–rays. Farther sources may have γ–rays attenuated by IR starlight. Neutrinos are not attenuated.

☆ AGNs may be the source of cosmic rays above the knee. The observation of neutrinos would provide strong confirmation.

☆ Neutron star binaries, such as Cyg X–3 and Her X–1 are now less promising.

☆ SN remnants may be observable for up to 10 years after the original blast.

☆ Perhaps SS433 and other galactic black hole binary candidate sources are mini–AGNs. They may be detectable.

☆ If the spectrum of γ–ray bursters should extend to the TeV region, and $\nu \approx \gamma$, they may be statistically detectable. This is a remote possibility.

☆ Some possibility exists for the detection of neutrinos from WIMPs (SUSY neutralinos) annihilating in the sun or earth. Negative results with large detectors will rule out significant portions of SUSY parameter space.

☆ Exotic sources of neutrinos such as the annihilation of cosmic strings or other topological defects are possible, though highly speculative.

7. Acknowledgements

Most of the work presented here has benefitted from the constructive criticism of many members of the DUMAND Collaboration. I would also like to thank Peter Biermann, Ray Protheroe, Paul Sommers, Todor Stanev, and Floyd Stecker for their valuable insights. And, of course, all the participants are all grateful to Leo Resvanis and his colleagues for a marvelous workshop in Pylos.

8. References

1. V. J. Stenger, 1991. DUMAND Internal Report DIR–16–91.

2. T.C. Weekes *et al. Astrophys. J.* **342,** 379 (1989); G. Vacanti *et al. Astrophys. J.* **377,** 467 (1991).

3. M. Punch *et al. Nature* **358,** 477 (1992).

4. J.G. Learned and V.J. Stenger, 1992. *High Energy Neutrino Astrophysics,* V.J. Stenger, J.G. Learned, S. Pakvasa, and X. Tata (eds), World Scientific Publishers. p. 288.

5. IAU *Circulars* 5431,5460, 5470, 5477, 5519 (1991/1992).

6. R.C. Hartman, *et al. Ap.J. Lett.,* **385**, L1 (1992).

7. M.F. Cawley *et al. Proc. 19th International Cosmic Ray Conference,* La Jolla, USA, 11–23 August, 1985, Vol. 1, p. 264.

8. F. W. Stecker, O. C. De Jager, and M. H. Salamon. *Ap J* **390**: L49 (1992).

9. See the Proceedings of the DUMAND workshops of 1976 and 1978, Hawaii DUMAND Center, Honolulu, Hawaii.

10. F.W. Stecker, C. Done, M.H. Salamon, P. Sommers. *Phys. Rev. Lett.* **66**, 2697 (1991).

11. A. Mastichiadis and J.G Kirk, 1992, *ibid.,* p. 63.

12. P. Sommers, 1992, *ibid,* p. 130.

13. Alexander Vilenkin and Eugene Chudnovsky, 1992, *ibid,* p. 151.

14. Marc Kamionkowski, 1992, *ibid,* p. 157.

15. P. Bhattacharjee, C. T. Hill, and D.N. Schramm, FERMILAB–PUB–91/304–A (1991).